AIAA JOURNAL
Vol. 30, No. 11, November 1992

Analysis of Fastened Structural Connections

Jacob Bortman* and Barna A. Szabó†
Washington University, St. Louis, Missouri 63130

An approach for modeling the transfer of forces in fastener groups is described which takes nonlinearities into account. The method is used for analyzing two problems which involve design of repairs and damaged structures. The model predictions are found to be in a good agreement with available experimental results. The study demonstrates the importance of fastener stiffness and initial clearance on load distribution.

I. Introduction

RELIABLE structural analysis of mechanically fastened connections is of major importance in modern design of aircraft structures where requirements for optimal design must be met. In current practice, extensive full-scale testing is used mainly because the reliability of mathematical models has not been established to the satisfaction of engineers who have to make or approve design decisions. Improved reliability of mathematical models will make it possible to reduce the scope of experimental programs and the time required for developing information on which design decisions can be based with confidence. Also, extensive testing programs can improve the safety of design (at a substantial cost) but cannot be used for optimizing design with respect to weight and durability. Only reliable mathematical models can do that.

In this paper, the problem of simulating the elastostatic response of fastened structural connections, with guarantee of reliability, is discussed. Some aspects of this problem were presented in Ref. 1 where the interaction between the fasteners and the plates was simulated by distributed springs. Friction was treated by the addition of external tractions in an iterative process. Each fastener was represented by a nonlinear relation between the transferred force and the relative displacements. The accuracy of the method was verified through tight quality control of the numerical approximation errors and comparisons with experimental results.

This paper is concerned with the accuracy and reliability of the mathematical model. Two kinds of error have to be considered[2]:

1) The differences between the exact solution of the mathematical problem formulated to represent a physical system and the actual response or behavior of the physical system are called errors of idealization.

2) The differences between the exact solution of the mathematical problem formulated to represent a physical system or process and its numerical approximation are called errors of discretization.

In some cases the two errors, the errors of idealization, and discretization may partially cancel one another. Therefore it is important to verify by means other than the experiment itself that the numerical solution is close to the exact solution of the model. Only then is it possible to investigate whether the errors of idealization are large or small by making comparisons with experimental observations.

The load distribution in bolted or riveted joints had been investigated both experimentally and theoretically, (e.g., Refs. 3–25). In these studies, a number of assumptions had been incorporated, such as ignoring friction, neglecting bending of fasteners, assuming uniform stress distribution in the plates at each section between any two adjacent rows, etc. Although these assumptions enable one to reduce the amount of effort required to obtain a load distribution among fasteners, one has to consider also the magnitude of error introduced by such simplifications. Understanding the effects of simplifications in terms of loss in accuracy and reliability is obviously of great importance.

Two model problems were investigated:

1) An orthotropic shear panel with a circular hold, simulating damage, repaired by an octagonal titanium plate.

2) A tensile orthotropic panel with a hole repaired by a trapezoidal titanium plate.

II. Nonlinear Model

The proposed nonlinear model is described in detail in Ref. 1; therefore only a brief review is given here. In the idealization process two structural entities are considered: First, the two sheets are defined as the first domain ($\Omega 1$) in which the linear two-dimensional elasticity relations are valid. In the following plane stress is assumed. Second, the fasteners ($\Omega 2$) are modeled by a combination of the elastic foundation theory with nonlinear relations (see Fig. 1). In the first step, the two layers are divided into a finite element mesh. The fasteners are idealized as follows: First, continuous distributed springs are attached to the perimeter of the fastener hole on one side and to a rigid disc on the other (see Fig. 1). This technique is used for modeling the contact stress between the fasteners and the plate. Second, a nonlinear relation between the relative displacements of the upper and the lower discs, which will be referred to as δ, and the load transferred by the fastener is specified. In this study the following relation was used for $\delta \geq \delta_0$:

$$\delta = P/A + B\,(P/P_j)^C + \delta_0 \tag{1}$$

where A, B, C, and P_j are the constants which characterize the fastener and δ is the initial clearance between the fastener and the hole. For $\delta \leq \delta_0$ the transferred force is set to zero.

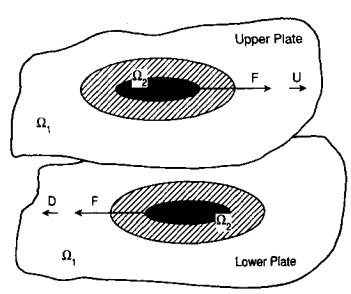

Fig. 1 Schematic representation of the model.

Received July 5, 1991; revision received May 11, 1992; accepted for publication May 11, 1992.

*Graduate Research Assistant, on leave from Israeli Air Force.

†Albert P. and Blanche Y. Greensfelder Professor of Mechanics and Director, Center for Computational Mechanics.

For the sake of simplicity the following definitions are introduced. First the upper and lower rigid disk displacements, as defined in Fig. 1, are arranged in a vector form, $\{U\}$ and $\{D\}$, respectively. Then the following linear relations are defined:

$$\{F\} = [S_{uu}]\ \{U\} \tag{2}$$

where the coefficient matrix $[S_{uu}]$ represents the relation between the displacements of the upper plate and the loads transferred by the fasteners $\{F\}$.

$$\begin{Bmatrix} Q_e \\ F \end{Bmatrix} = \begin{bmatrix} [S_{ee}] & [S_{ed}] \\ [S_{de}] & [S_{dd}] \end{bmatrix} \begin{Bmatrix} D_e \\ D \end{Bmatrix} \tag{3}$$

where $[S_{ee}]$ relates the external force Q_e to the displacement at the applied load zone D_e. The vector $[S_{ed}]$ and the matrix $[S_{dd}]$ are defined in a similar fashion.

These coefficient matrices, which represent the mechanical response of the repair and the panel, were computed by the finite element program MSC/PROBE[26]. Superconvergent procedures were employed for computing the total force transferred by the fasteners and the stress intensity factors. This allows for a very substantial reduction in the number of degrees of freedom. To further reduce computing resource requirements, and thus to decrease solution time, the linear degrees of freedom are first condensed out and then the "hybrid method" developed by Powel[27] is implemented to solve the nonlinear equations.

III. Repair of a Composite Panel—Shear Loading

The first problem considered is typical for repairs of composite panels subjected to shear loading: A composite panel with a 63.5-mm (2-1/2 in.)-diam circular hole, simulating damage, and three metal reinforcements, is loaded by a stiff frame which imposes a shear-dominant loading. The damage was repaired by an octagonal titanium plate designed to relieve the highly stressed area in the neighborhood of the damage. The panel was tested and strains were recorded at three locations. The panel geometry with its relevant dimensions and the three strain gauge locations are shown in Fig. 2. Experimental results for this test are available in Ref. 16. Since the panel is loaded primarily in shear, the laminate layup contains a high percentage of ± 45 deg graphite/epoxy tape plies (AS-1/3501-6 G/E). The layup is [± 45, 0, ± 45, 90 deg]$_s$ with a thickness of 1.981 mm (0.078 in.) The equivalent homogenous material properties for the laminate were calculated in Ref. 16 to be $E_x = 33.58$ GPa $(0.487 \times 10^7$ psi), $E_y = 28.68$ GPa $(0.416 \times 10^7$ psi), $\nu_{xy} = 0.604$, and $G_{xy} = 26.20$ GPa $(0.380 \times 10^7$ psi). These equivalent orthotropic properties were determined using the classical thin lamination theory, in which the laminate is assumed to consist of perfectly bonded laminae. Moreover, the bonds were assumed to be infinitesimally thin as well as nonshear-deformable (no slippage between layers). Thus, the laminate acts as a single layer of material with effective properties[28].

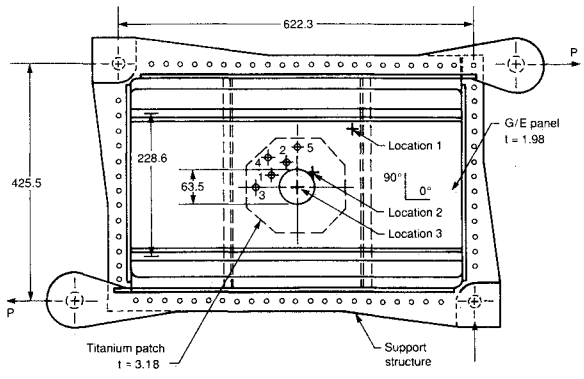

Fig. 2 Bolted repair shear test (dimensions in millimeters; Ref. 16).

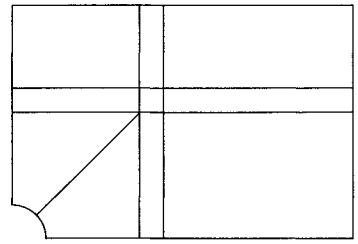

Fig. 3 Finite element mesh used for analyzing the unrepaired panel.

The test procedure included two main steps: In the first one, the damaged panel had been tested without the titanium repair. In the second step, after installing the repair, the panel was loaded again, this time to failure. In both cases strain measurements were recorded during the loading.

A. Previous Analytical Work

One of the better models for quantifying the error of idealization of fastened connections was developed within the framework presented in Ref. 15 and in more detail in Ref. 16. This model was created for analyzing tapered-width orthotropic repair patches bolted to a skin of finite width with a centrally located damaged hole. The derivation is based on compatibility of displacements at the fastener location while allowing for fastener flexibility and clearance. The patch and skin displacements are related to the forces by influence coefficients which are determined using boundary integration and boundary collocation. Two superelements, the skin and the patch, are modeled using series expansions that describe the displacement and stress fields within each element. Unit loads, cosine-distributed at each of the bolt holes, were used in developing a set of equations to determine the bolt loads.

This model, like all models restricted to linear relationships, incorporates certain assumptions which do not represent the real behavior of fastener groups well: First, the superposition of the x component and the y component of the influence coefficients is not accurate. This can be resolved by iteration by first solving for the load direction and then obtaining the influence coefficient based on this direction. Second, since the model includes the effects of initial clearance, the force-displacement relation describing the fastener cannot be a linear function. Different relations should be used in three regions, for the relative displacement δ such as 1) $\delta > \delta_0$, in which a linear relation, $F = b_0 \cdot (\delta - \delta_0)$ should be assumed, where b_0 is the fastener stiffness, F is the transferred force and δ_0 is the initial clearance; 2) $-\delta_0 \le \delta \le \delta_0$, in which the transferred force is zero; and 3) $\delta < -\delta_0$, in which the linear relation should be of the type $F = b_0 \cdot (\delta + \delta_0)$ (note that the initial clearance δ_0 reversed its sign). Third, nonlinear effects such as frictional loads, plasticity, and contact are not considered.

In the following formulation of a nonlinear model which accounts for both the force and stress distribution in fastened structural connections, provided that the effects of out of plane bending can be neglected, is outlined.

B. Present Analysis of the Unrepaired Panel

The p-version finite element code MSC/PROBE was used for analyzing this test case. The two stiffeners were represented in the model by increasing the effective thickness in the required zones (see Fig. 2). The mesh is shown in Fig. 3. Taking advantage of antisymmetry, only a quarter of the specimen was analyzed.

Two different boundary conditions were considered and compared: a) Model A: The loading was applied through uniformly distributed normal traction; and b) Model B: The loading was applied through uniformly distributed displacement. The panel began to buckle at the edge of the hole when the external applied load was just above 35.58 kN (8000lb). To stay within the linear range, the comparison between the cur-

rent finite element predictions and the test results was made for the 35.58 kN (8000 lb) load. Table 1 contains comparisons between the shear strain γ_{xy} at location 2, the maximum principal strain at location 1 with the reported test data. Analysis results based on the boundary collocation and boundary-integration methods[15] are also presented in Table 1. Both analytical predictions are in close agreement with the reported test data. As was expected, the second model, model B, in which uniform displacement was imposed, agrees better with the test results. To reduce test inaccuracies, strains were measured at different locations which were expected to show the same values (i.e., back to back and antisymmetric points). Table 1 presents average and extreme test measurements taken from Ref. 16.

C. Present Analysis of the Repaired Panel

Following the unrepaired test case, a 3.175-mm (0.125 in.)-thick 6AL-4V titanium patch was installed on the specimen with sixteen 4.763-mm (3/16 in.)-diam Jo-Bolts. The numbering for five bolts is shown in Fig. 2. Two finite element models were considered. One for the panel (the lower plate) and the other for the titanium repair (the upper plate). Both models include the fastener holes. The meshes are shown in Fig. 4. The fasteners were represented by distributed springs with a stiffness of $2.5/d\ E_{\text{titanium}}$, where d is the fastener diameter. The three-parameter model was employed for describing the fastener behavior. The relationship between the relative displacement δ of the upper and the lower rigid disks and the load transferred F was constructed using Eq. (1). The required parameters are documented in Ref. 16 as follows: $A = 22.45$ kN/mm (0.1282×10^6 lb/in.), $B = 0$, and $\delta_0 = 0.0508$ mm (0.002 in.).

In the first step, coefficient matrices for the upper plate and lower plate, $[S_{uu}]$ and $[S_{dd}]$, the vector $[S_{ed}]$, and the scalar S_{ee} were computed. These coefficient matrices are defined in the global xy-coordinate system. Each fastener is represented by two degrees of freedom, x and y, as shown in Fig. 5. Finally, for each required parameter (e.g., strain), a coefficient matrix for unit fastener displacement was extracted. In this case the strain level at three locations was considered. Then the above data was used to obtain the load distribution between the fasteners (magnitude and direction) which is documented in Tables 2 (magnitude) and 3 (angle). At this point, the relative displacement between the upper rigid disks and the lower rigid disks ($\bar{\delta} = \bar{U} - \bar{D}$) is not necessarily in the same direction as that of the transferred load. Using the method described in Ref. 1, the direction of the transferred load was evaluated. In this first step, the initial clearance was set to zero to eliminate possible conflict in the direction between the load and the relative displacement. Then, a second iteration was performed in which the xy degrees of freedom were rotated to coincide with the resultant load direction $\hat{n}$, as shown in Fig. 5. The modified matrices were used for computing the load distribution among the fasteners. As could be expected, the change in the direction of the transferred load was found to be relatively small (i.e., in all cases the transverse component F_t was negligible relative to the normal component F_n). In this case for all fasteners, the transferred force and the relative displacement

Table 1 Comparison between the analysis results and test measurements—before installation of the repair (the strains are given in μmm/mm)

Strain gauge	Test results[b]	Ref. 15 predictions	Current model	
			Model A	Model B
γ_{xy} at 1[a]	785^{+68}_{-85}	912 (16%)	894 (14%)	861 (9.7%)
$\epsilon_{\theta\theta}$ at 2[a]	1700^{+274}_{-310}	1740 (2.4%)	1768 (4%)	1690 (0.6%)

[a]Locations at 1 and at 2 are defined in Fig. 2. [b]Taken from Ref. 16.

Table 2 Fastener forces. Comparison between the current model with Ref. 15 [forces are in Newtons (lb)]

Fastener no.	Ref. 15	Current model	
		First iteration[a]	Second iteration
1	1824 (410)	2366 (532)	1886 (424)
2	1784 (401)	2344 (527)	1859 (418)
3	1508 (339)	2224 (500)	1557 (350)
4	2282 (513)	2669 (600)	2349 (528)
5	1490 (335)	2286 (514)	1619 (364)

[a]In the first iteration the initial clearance is set to 0.

Table 3 Orientation of fastener forces. Comparison between the current model and Ref. 15 (angles are in degrees measured from the x axis)

Fastener no.	Ref. 15	Current model
1	59.0	59.2
2	31.0	30.3
3	90.0	90.0
4	44.8	44.5
5	0.0	0.0

Table 4 Comparison between test results and analysis (the strains are reported in μmm/mm)

Strain gauge	Test results	Ref. 15 predictions	Current model	
			First iteration	Second iteration
γ_{xy} at 1[b]	3721^{+548}_{-447}	3800 (2.1%)	3932 (5.6%)	3834 (3.0%)
$\epsilon_{\theta\theta}$ at 2[b]	$4507.5^{+140.5}_{-140.5}$	4371 (3.0%)	3759 (17.0%)	4268 (5.3%)
γ_{xy} at 3[b]	$910^{+1556[a]}_{-1556}$	822 (9.7%)	990 (8.8%)	797 (12.4%)

[a]The large scatter makes the test results questionable at location 3.
[b]Locations at 1, at 2, and at 3 are defined in Fig. 2.

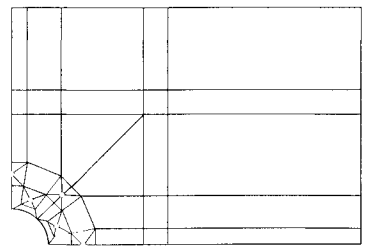

a) Lower plate—composite panel

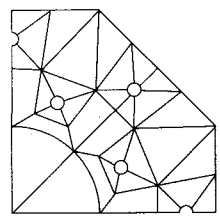

b) Upper plate—titanium patch

Fig. 4 Finite element meshes used for analyzing the repaired panel.

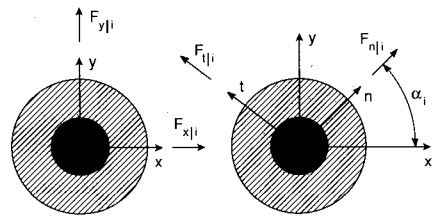

Fig. 5 Fastener degrees of freedom.

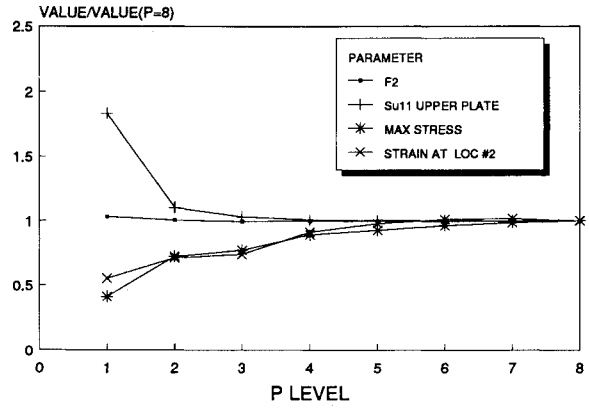

Fig. 6 Shear panel—convergence study.

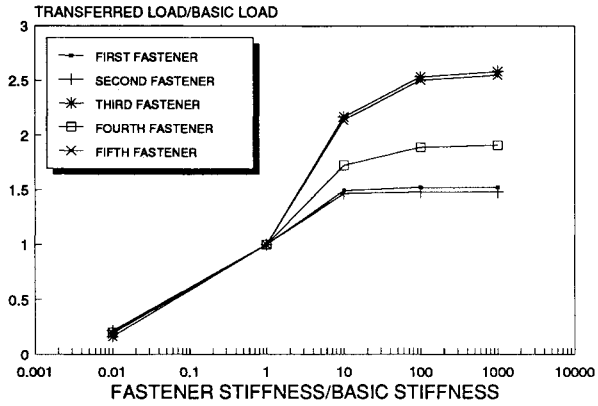

Fig. 7 Transferred loads for different fastener stiffnesses.

are in the same direction. The forces calculated in this second iteration are presented in Table 2.

A comparison between the strains predicted by the current model and the test results are presented in Table 4. The comparison was made for the external load level of 133.4 kN (30,000 lb). As was expected, the second iteration gave better predictions than the first one. The results for the first two locations are in good agreement with the test results while for the third location the difference is 12.4% which can be explained by the large scatter (170%) in the test measurements for this location.

It is concluded that the correlations are generally good, considering the presence of various error contributions such as buckling and gauge placement. Table 2 also includes comparisons between the transferred forces from the analysis of Ref. 15 and the current model. Again, the results are close.

D. Convergence Study

It is necessary to verify that the numerical solution is close to the exact solution of the mathematical model. In the current model, the p-version of the finite element method was employed to extract the coefficient matrices, then the load distribution was calculated and, finally, stresses and strains were obtained. The convergence of each of these parameters was investigated. Figure 6 includes representative normalized data for the different parameters, with respect to the most accurate solution available which, in this case, is for $p = 8$.

First, the convergence of the coefficient matrices was studied. As an example, the results for $S_{uu}(1,1)$ are plotted in Fig. 6 against p level. For $p > 4$, the estimated error for this term is less than 2% relative to $p = 8$. This fast rate of convergence is due to a superconvergent method of extraction employed. Second, the convergence of the load distribution among the fasteners was examined. The transferred load by the second fastener is plotted in Fig. 6. In this case, it was found that convergence is even faster. Finally, strain and stress convergence were studied. As could be expected, in this case the rate of convergence is slower. The strain ($\epsilon_{\theta\theta}$) at location 2 converged somewhat faster than the maximum stress, which was found to be at location 4, on the perimeter of the fourth fastener hole of the panel. Again, the data is presented in Fig. 6. Based on these results, it is concluded that in order to study the load distribution among the fasteners it is sufficient to use $p = 5$, but for strains and stresses higher p levels (up to $p = 8$) are required.

E. Parametric Studies

To understand the sensitivity of the results to different fastener parameters, a parametric study was performed. Two parameters were investigated: first the initial clearance, and second the fastener stiffness.

1. Initial Clearance

Since the exact initial clearance at each fastener cannot be measured in practical cases, it is important to assess the sensitivity of the results to changes in initial clearance. Five different cases were solved, where an increase of 0.0254 mm (0.001 in.) in clearance was assigned to each of the fasteners, one fastener at a time. The percent change in the load distribution among the fasteners for each increase in clearance (as well as in the strains at locations 1, 2, and 3) relative to the basic case, where the initial clearance was set to 0.0508 mm (0.002 in.) in all of the fasteners, are reported in Table 5. In all cases, the load transferred by the fastener whose clearance was increased by 0.0254 mm (0.001 in.) was found to decrease by 15–18%. The strains were found to be most sensitive to a change in the fourth fastener, which is due to the fact that in the basic case this fastener carries the largest load. The strain at location 2 becomes larger when the initial clearance is increased. This can be explained by the fact that the transferred forces are reduced and less relief is given to the highly stressed zone in the panel by the titanium repair. The same argument can be used to explain why the shear strain in the repair (location 3) is reduced.

In all cases, the fastener load is most sensitive to its own level of clearance. The fourth fastener is affected very little by changes in clearance levels in other fasteners, and when the initial clearance at this fastener is increased, the additional load is equally distributed among the fasteners. This is an important fact which makes the situation less critical. If the other fasteners were installed with a higher initial clearance, the additional load would be distributed among the other fasteners and only a small amount of that load would be carried by the fourth fastener which is originally the most critical. Note that relief forces from the inner fasteners (1 and 2) are moved to the external fasteners (3 and 5); loads from the external fasteners are first moved to the other external fastener (excluding fastener 4) and only then to the inner fasteners. This fact explains the nature of the repair—when the symmetry is disturbed, the fasteners which are remote from the

Table 5 Percent change in transferred load and strains as a result of a 0.0254 mm (0.001 in.) increase in initial clearance

	Fastener number with increased clearance				
Parameter	1	2	3	4	5
F1	−17.2%	−0.5%	4.2%	3.4%	−2.7%
F2	−0.5%	−17.6%	−2.8%	3.5%	4.3%
F3	12.4%	−4.6%	−15.3%	3.8%	−7.9%
F4	2.7%	2.8%	0.6%	−16.2%	0.6%
F5	−6.2%	9.8%	−9.3%	1.9%	−16.5%
γ_{xy} at 1[a]	−0.29%	−0.31%	0.05%	−0.81%	0.08%
$\epsilon_{\theta\theta}$ at 2[a]	−1.56%	−1.48%	0.68%	1.87%	0.68%
γ_{xy} at 3[a]	−0.04%	−0.04%	−0.29%	−4.44%	−0.20%

[a]Locations at 1, at 2, and at 3 are defined in Fig. 2.

symmetry line are the first ones to be affected, as the corresponding moment arms are the largest.

2. Fastener Stiffness

An important parameter which controls the amount of load transferred from the panel to the repair is the stiffness of the fasteners. To study the sensitivity of the load distribution with respect to fastener stiffness, five additional levels of stiffness were solved in the range $0.01b_0$ to $1000b_0$, where b_0 is the basic fastener stiffness. The load distribution among the fasteners for each case is reported in Fig. 7. The external fasteners (3 and 5) are more heavily loaded relative to the inner fasteners when the fastener stiffness is increased.

IV. Repair of a Composite Panel—Tensile Loading

The second test case considered is a damaged panel made of graphite/epoxy repaired by a mechanically fastened titanium patch. The repaired panel is loaded in tension. The proposed model was employed to solve this second case.

A composite laminate with a 101.6-mm (4.0 in.)-diam hole simulating damage near a spar and a rib, as shown in Fig. 8, is loaded in tension. The graphite/epoxy laminate was fabricated from AS/3501-6 tape with a [0, ± 45, 90] layup pattern to a thickness of 12.7 mm (0.5 in.). Using the classical thin lamination theory, the equivalent homogenous material properties for the laminate were calculated in Ref. 15 to be $E_x = 68.96$ GPa (1.0×10^7 psi), $E_y = 26.62$ GPa (0.386×10^7 psi), $G_{xy} = 17.65$ GPa (0.256×10^7 psi), and $\nu_{xy} = 0.548$. The

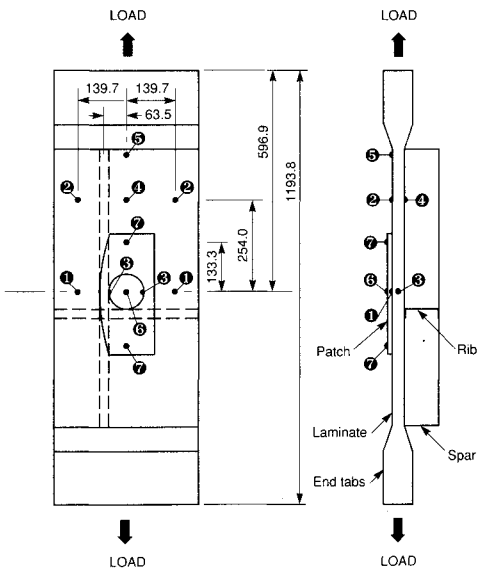

Fig. 8 Repaired panel test case—tension (dimensions in millimeters).

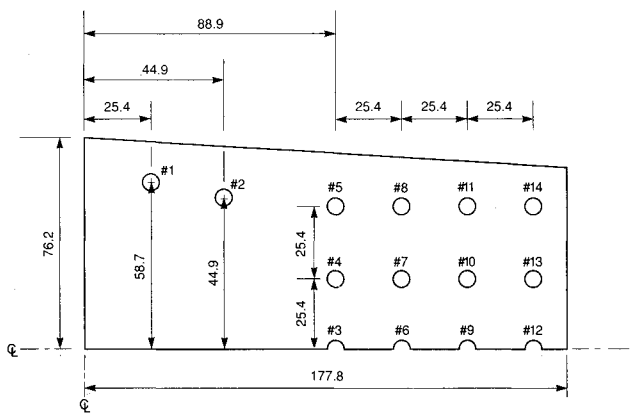

Fig. 9 Idealization of the titanium patch (dimensions in millimeters).

Table 6 Comparison of the test results for the strains with analytical results

Location	Test[a]	Ref. 15[a]	Current model[a]
1	3830	4064	3915 (2.2%)
2	3639	3890	3973 (9.2%)
3	10822	10626	10207 (−5.7%)
4	3491	4066	4011 (14.9%)
5	4000	—	4024 (0.6%)
6	2617	3839	2818 (7.7%)
7	959	992	1014 (5.7%)

[a]Strains are given in μmm/mm.

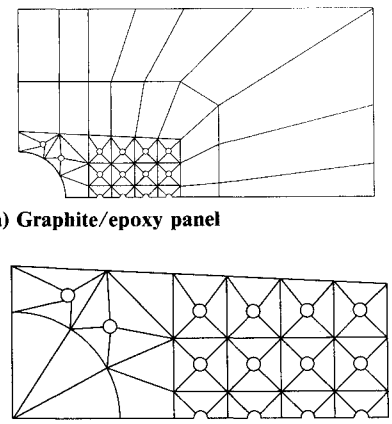

a) Graphite/epoxy panel

b) Titanium repair

Fig. 10 Finite element meshes for the panel and the repair—the tension case.

damage was repaired by a titanium plate designed to reduce stresses in the neighborhood of the damage. The repair and numbering scheme used for 14 of the fasteners are shown in Fig. 9. The 4.064-mm (0.16 in.)-thick titanium patch was attached by a total of 48 6.35-mm (0.25 in.) Jo-Bolts to the test specimen.

Loading plates were bolted to each end of the repair specimen and attached to the test machine with a single pin joint at each end to impose a tension-dominant field. Figure 8 shows the locations of the strain gauges installed on the specimen. The specimen was subjected to an initial load of 266.8 kN (60 kips) to seat the load plates and to calibrate the strain gauges. The specimen was then loaded in increments of 266.88 kN (60 kips) to test ultimate load with strain data recorded at each increment. The results are documented in Table 6 for a load of 1.36 MN (305.9 kips). This load level corresponds to approximately 4000 μmm/mm gross laminate strain. Geometric details are given in Figs. 8 and 9.

A. Analysis

Since most of the geometric details are almost symmetric with respect to two planes of symmetry, it was decided to analyze a quarter of the specimen and to impose boundary conditions of symmetry along the lines of symmetry. Two finite element meshes were constructed: one for the graphite/epoxy panel, the other for the titanium repair. The meshes are shown in Fig. 10. The fasteners were represented by distributed springs with a stiffness of $2.5/d\ E_{\text{titanium}}$, where d is the diameter. Again, the three-parameter model was employed to describe the relation between the transferred force and the relative displacement (1). The three constants A, B, C, and δ_0 for this case are given in Ref. 16 as follows: $A = 81.95$ kN/mm (0.468×10^6 lb/in.), $B = 0$, $C = 1.0$, and $\delta_0 = 0.0508$ mm (0.002 in.).

Next the upper and lower plate coefficient matrices, $[S_{uu}]$ and $[S_{dd}]$, the vector $[S_{ed}]$, and the scalar S_{ee} were extracted.

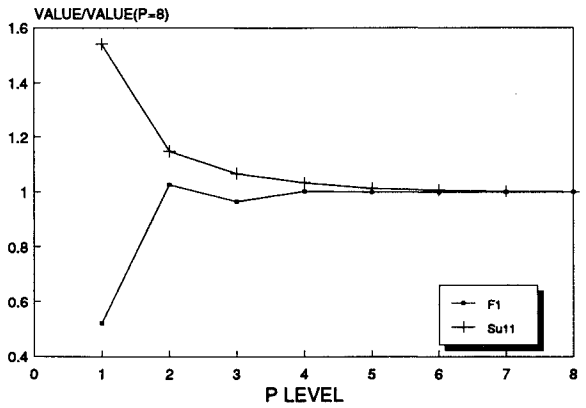

Fig. 11 Convergence study—the tension panel.

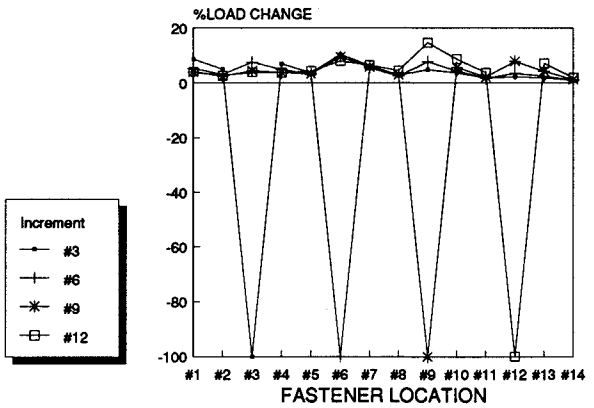

a) Increment of 0.254 mm (0.01 in.) in initial clearance

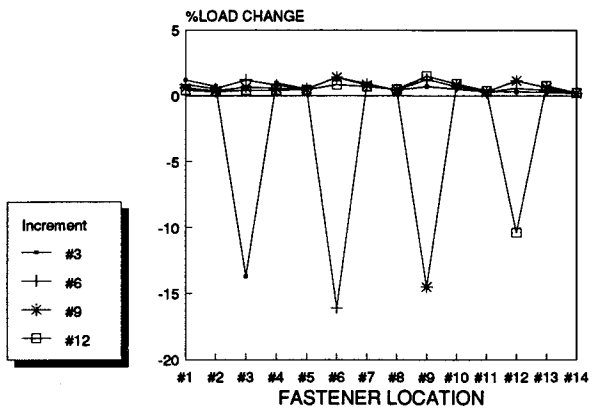

b) Increment of 0.0254 mm (0.001 in.) in initial clearance

Fig. 12 Effect of increasing the initial clearance.

Furthermore, for each strain-gauge location, a coefficient matrix, for a unit fastener displacement, was extracted. The above data was then employed in calculating the rigid disk displacements as well as the load distribution among the fasteners. As with the shear panel case, two iterations were necessary to solve first for the load direction and then for the actual loads and displacements. Finally, using the above coefficient matrices, the strains at the seven locations were calculated. The comparison between the strains predicted by the current model and the test results are presented in Table 6. The comparison is made for an external load of 1.36 MN (305.9 kips). The results for most of the locations are in a good agreement with the experimental test results. Only for the fourth location is the difference greater than 10%. This disagreement can be explained by the fact that the configuration is not symmetric (the repair is installed only on one side of the panel) which probably caused the specimen to bend. This bending resulted in reduced tensile strains on the patch outer surface.[16] As the current model is two-dimensional, it does not account for bending but only for the average (membrane) strain through the thickness. This is a modeling error which can be eliminated by using a computationally more demanding plate model for the panel and the repair.

B. Convergence Study

As previously noted, it is important to verify that the finite element solution is substantially independent of the discretization. A convergence study was performed for this purpose. Figure 11 presents representative normalized data for one of the terms in the coefficient matrix $S_{uu}(1, 1)$ and for the force transferred by the first fastener F_1. The data is normalized with respect to the most accurate solution available ($p = 8$). In both cases, for $p > 4$ the estimated error is less than 2% relative to $p = 8$. As in previous cases, the transferred load F_1 showed a somewhat greater convergence rate than the coefficient matrix term $S_{uu}(1, 1)$. It is again concluded that in order to study the load distribution among fasteners, it is sufficient to use $p = 5$.

C. Parametric Studies

As in the case of the shear panel, in order to investigate the sensitivity of the results to variations in fastener parameters, a parametric study was conducted. Again, the following two parameters were studied: 1) the initial clearance, and 2) the fastener stiffness.

1. Initial Clearance

The sensitivity of the load distribution to changes in the initial clearance was investigated. First, an increase of 0.0254 mm (0.001 in.) in clearance was specified for each fastener, one fastener at a time, along the center row (fasteners #3, #6, #9, and #12 as defined in Fig. 9). The percent change in the transferred load is presented in Fig. 12a. Then an increase of 0.254 mm (0.01 in.) was specified at the same locations. The results of this study are shown in Fig. 12b. Note that in both cases the behavior is similar: the fasteners located in the neighborhood of the fastener with the increased clearance absorbed more of the relieved load than the other fasteners. The load transferred by the fasteners with larger clearances decreased 10–40% for the 0.0254-mm (0.001 in.) clearance level and 100% for the 0.254-mm (0.01 in.) clearance level.

2. Fastener Stiffness

The second parameter investigated is the effect of variations in fastener stiffness. Six additional stiffness values were considered in the range $0.001b_0$ and $1000b_0$, where b_0 is the basic fastener stiffness, 81.95 kN/mm (0.468×10^6 lb/in.). The normalized transferred load by each of the fasteners in the center row (fasteners #3, #6, #9, and #12) is shown in Fig. 13. In this case, the two extreme fasteners (#3 and #12) transfer more of the load when the fasteners become stiffer while the inner ones

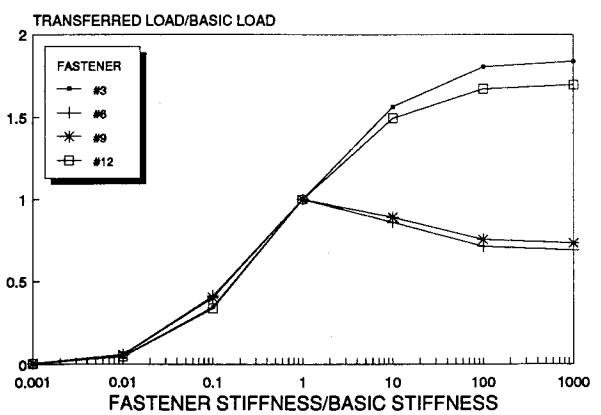

Fig. 13 Transferred load for different fastener stiffnesses.

(#6 and #9) transfer less load than they did originally. In this case, the "saturation point" is found to be close to $100b_0$. From this point on the load is virtually insensitive to change in the fastener stiffness.

V. Summary and Conclusions

Numerical solutions were obtained by means of the p-version of the finite element method. The solution process involved two steps: First, linear coefficient matrices were obtained using the p-version finite element code MSC/PROBE. Second, the nonlinear equations were solved by a program especially written for that purpose.

The model predictions were found to be in a good agreement with the experimental results reported in the literature. In all cases, quality control and error estimation calculations based on p-extensions were performed. Based on these model problems, it was concluded that for load analysis relatively coarse mesh can be used with $p \leq 5$. For strain and stress analyses, as well as for fracture mechanics computations, higher p-levels are needed, however.

Based on previous investigations, and on the current study, it was found that there are two important parameters which affect the load distribution among the fasteners (these could be determined with a relatively low level of confidence): the fastener stiffness and the level of initial clearance at each fastener. Both of these parameters are controlled by the manufacturing and the installation processes. Based on representative cases the following observations are made:

1) It was found that in all cases there were two saturation points with respect to the fasteners' stiffness, called the "weak" and "stiff" points, beyond which the fasteners may be considered as infinitely weak or stiff, respectively. To understand the sensitivity of the loads with respect to fastener stiffness, one should first locate the investigated case relative to these two points.

2) Two increments of initial clearance were specified. A high level (relative to the original displacement) to represent a poor installation where the fastener may be considered almost absent, and a low level which corresponds to a minor flaw in installation. In both cases, the behavior was found to be similar: for the tensile cases, the largest load change was always at the fastener location where the increment of clearance was specified, and the load change decayed with the distance from that fastener. For the shear case, moment considerations controlled load redistribution.

Acknowledgments

The first author wishes to thank the Israeli Air Force for support of his research. The second author wishes to acknowledge partial support received from the Air Force Office of Scientific Research through research Grant 88-0017 and from the National Science Foundation through research Grant DDM-8917736.

References

[1]Bortman, J., "Nonlinear Models for Fastened Structural Connection Based on the p-Version of the Finite Element Method, D.SC. Dissertation, Dept. of Mechanical Engineering. Washington Univ., St. Louis, MO, 1991.

[2]Szabó, B., and Babuška, I., *Finite Element Analysis*, Wiley, New York, 1991, Chap. 16.

[3]Barrois, W., "Stress and Displacements due to Load Transfers in Structural Assemblies," *Engineering Fracture Mechanics*, Vol. 10, No. 1, 1978, pp. 115–176.

[4]Batho, C., "The Partition of Load in Riveted Joints," *Journal of the Franklin Institute*, Vol. 182, No. 5, 1916, pp. 553–604.

[5]Tate, M. B., and Rosenfeld, S. J., "Preliminary Investigation of the Loads Carried by Individual Bolts in Bolted Joints," TN 1051, NACA, Washington, DC, May 1946.

[6]Rosenfeld, S. J., "Analytical and Experimental Investigation of Bolted Joints," TR TN 1458, NACA, Washington, D.C., Oct. 1947.

[7]Vogt, F., "The Load Distribution in Bolted or Riveted Joints in Light-Alloy Structures," Royal Aircraft Establishment, TR TM 1135, (RAE Rept. SME 3300), NACA, Washington, DC, April 1947.

[8]Cramer, C. O., "Load Distribution in Multiple-Bolt Tension Joints," *Journal of the Structural Division, ASCE*, Vol. 94, ST5, 1968, pp. 1101–1117.

[9]McCombs, W. F., McQueen, J. G., and Perry, J. L., "Analytical Design Methods for Aircraft Structural Joints," Air Force Flight Dynamics Laboratory, TR AFFDL-TR-67-184, LTV Aerospace, Dallas, TX, Jan. 1968.

[10]Rumpf, J. L., "The Ultimate Strength of Bolted Connections," Ph.D. Thesis, Dept. of Civil Engineering, Lehigh Univ., Bethlehem, PA, 1960.

[11]Bendigo, R. A., Hansen, R. M., and Rumpf, J. L., "Long Bolted Joints," *Journal of the Structural Division, ASCE*, Vol. 89, ST6, 1963, pp. 187–213.

[12]Vasarhelyi, D. D., and Chen, C. C., "Bolted Joints with Plates of Different Thickness," *Journal of the Structural Division, ASCE,* Vol. 93, ST6, 1967, pp. 201–211.

[13]Yen, S. W., "Investigation of Load Distribution Among Fasteners in a Multiple Row Double-Cover Butt Joint," Douglas Aircraft, TR MDC-J5049-01, Long Beach, CA, July 1971.

[14]Yen, S. W., and Smillie, D. G., "Computer Analysis of Fastener Load Distribution in a Multi-Row Joint," *Computers and Structures*, Vol. 3, No. 4, 1973, pp. 1293–1320.

[15]Bohlmann, R. E., Renieri, G. D., and Libeskind, M., "Bolted Field Repair of Graphite/Epoxy Wing Skin Laments," *Joining of Composite Materials,* edited by K. T. Kedward, ASTM STP 749, American Society for Testing and Materials, Philadelphia, PA, pp. 97–116.

[16]Bohlman, R. E., Renieri, G. D., and Horton, D. K., "Bolted Repair Analysis Methodology," McDonnell Douglas, TR NADC-81063-60, St. Louis, MO, 1982.

[17]Swift, T., "The Effects of Fastener Flexibility and Stiffener Geometry on the Stress Intensity in Stiffened Cracked Sheet," *Proceedings of an International Conference on Prospects of Fracture Mechanics*, edited by G. C. Sih, H. C. van Elst, and D. Broek, Noordhoff International Publishing Leyden, Groningen, The Netherlands, 1974, pp. 417–436.

[18]Swift, T., "Fracture Analysis of Stiffened Structures, *Damage Tolerance of Metallic Structures: Analysis Methods and Application,* edited by J. B. Chang and J. L. Rudd, ASTM STP 842, American Society for Testing and Materials, Philadelphia, PA, 1984, pp. 69–107.

[19]Bortman, J., "Nonlfas—Code Documentation," Washington Univ., TR WU/CCM-90/3, St. Louis, MO, 1990.

[20]Low, M. C., and Cartwright, D. J., "Fracture Diagrams for Stiffened Aircraft Structures: Effects on Material Nonlinearity," *Durability and Damage Tolerance in Aircraft Design*, edited by A. Salvetti, International Committee on Aeronautical Fatigue, Chameleon Press, London, 1985, pp. 550–603.

[21]Swift, T., "Repairs to Damage Tolerance Aircraft," *Proceedings of an International Symposium on Structural Integrity of Aging Airplanes*, (Atlanta, GA), March 1990, pp. 433–483.

[22]Kuo, A., Yasgur, D., and Levy, M., "Assessment of Damage Tolerance Requirements and Analyses—Task i Report," Air Force Wright Aeronautical Laboratories, TR AFWAL-TR-86-3003, Fairchild Republic, March 1986.

[23]Shkarayev, S. V., and Moyer, E. T., "Edge Crack in Stiffened Plates," *Engineering Fracture Mechanics*, Vol. 27, No. 2, 1987, pp. 127–134.

[24]Wang, S., and Han, Y., "Finite Element Analysis or Load Distribution of Multifastener Joints," *Journal of Composite Materials*, Vol. 22, Feb. 1988, pp. 124–135.

[25]Tong, P., Greif, R., and Chen, L., "Application of Hybrid Finite Element Method to Aircraft Repairs, *Proceedings, 22nd Fracture Mechanics Symposium*, (Atlanta, GA), American Society of Testing and Materials, Philadelphia, PA (to be published).

[26]Szabó, B., *PROBE: Theoretical Manual, Release 1.0,* Noetic Technologies, St. Louis, MO, 1985.

[27]Powell, M. J. D., "A Hybrid Method for Nonlinear Equations," edited by P. Rabinowitz, *Numerical Developments in Solving Nonlinear Algebraic Systems*, edited by P. Rabinowitz, Gordon and Breach, New York, 1970, pp. 87–114.

[28]Jones, R. M., *Mechanics of Composite Materials,* Scripta, Washington, DC, 1975, pp. 147–187.